Numerical Simulation of Cold Air Distribution in the Room with Different Supply Patterns

Prof.Sabah Tarik Ahmed
University of Technology
Mechanical Eng. Dept.

Ass. Prof.Ala'a Abbas Mahdi
University of Kufa
College of Engineering

Eng. Hyder M. Abdul Hussein
University of Kufa
College of Engineering

ABSTRACT
In this paper three-dimension turbulent buoyant cases of heat transfer and air flow has been presented for enclosed cooling space. Experimental study is carried out to validate the numerical simulations, and the predictions are performed by means of the Realizable k-ε and SST k-ω models by performing simulations on FLUENT 6.3.26. Comparisons between the predictive results and the experimental data reveal that both of the tested turbulence models are capable of capturing the main qualitative flow features satisfactorily.

The airflow in a room ventilated by displacement diffuser, slot diffuser, square diffuser, and grille diffuser is calculated by the simplified system, respectively. Comparing calculated results to measured data, it is clear that the simplified methodology can predict indoor airflow and temperature gradient with satisfactory results for engineering applications.

Keywords
Numerical simulation, cold air distribution, temperature profile, velocity profile, Different Supply Patterns

1. INTRODUCTION
That the study of the air distribution in enclosed spaces design aspects of the task is to reduce the energy expended to energy consumption and find out suitable climates for people means that a state of thermal comfort has to be achieved on the one hand and the equipment inside spaces on the other hand. Provide the proper climate balance, which concerns people the occupants of a place several values is the speed of the air, the distribution of air temperature, humidity, contaminants, surface temperature of surrounding walls, windows and heating surfaces the ratio of carbon dioxide.

The CDF method of modeling for air diffusers various programs easy way for researchers to knowledge predict the movement of air flow, and all parts must be calculated is included in the internal space to be studied in terms of furniture and appliances.

Many researchers has studied to predict in terms of air diffusers or in terms of the movement of air and temperature distribution within the enclosed space and we review them as, "Skovgard and Nielsen (1991), Moser 1991, Zhang et al. 1992, Vogel et al. 1993, Regard et al. 1995, and Jacobsen and Nielsen 1993 Cehlin et al. (2010) modeling the airflow supplied from the diffuser as a major limiting factor in applying CFD to room airflow",[1,2,3]. and Zhao et al. (2003) used "N-point air supply opening model" is applied to describe boundary conditions of air terminal devices in computational fluid dynamics calculation. They concluded that the box method had better performance, however, this depends on the diffuser-specific data[4]. There are recent studies now theoretical and experimental form of distribution of contaminants as lee et. al. (2009) and Tung et al. (2009) where focused in positive or negative pressure inside the room,[5,6]. Some recently researches as Gharbi et al. (2011) were studied Effect of Different Near-Wall Treatments to obtained a good prediction with the aid of CFD code,[7].

In this work has been to focus on a case study on four types of modeling the most important publisher is (slot (linear) diffuser, displacement diffuser, square ceiling diffuser and grille diffuser) used in the study to the ASHRAE RP-1009 [5] and helpful to measure the results of experimental results measured to be compared with the analysis by CFD, This work was in the modeling of the test chamber to give true behavior with similar indoor furniture and appliances.

2. PHYSICAL MODEL
This subject took an experimental air-conditioned room as a simulative object. The size of the room is (5.16 m) long, (3.65 m) wide, and (2.43 m) high. In Figure 1 shows how the diffusers were installed in an environmental chamber.

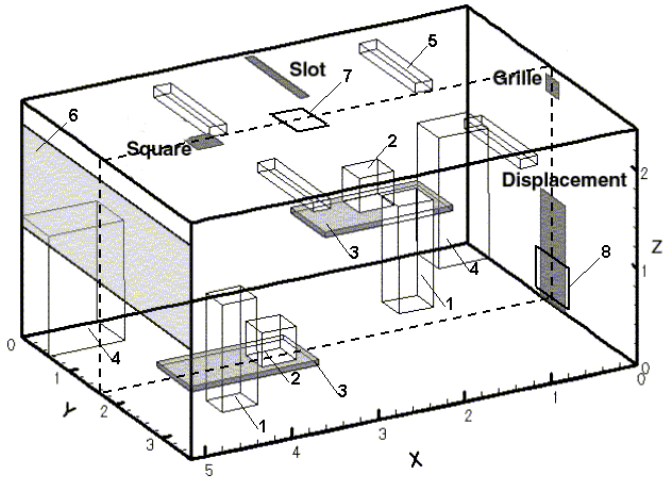

Figure 1. Element of test room and positions of the supply diffusers (person - 1, computer - 2, table - 3, cabinet - 4, fluorescent lamp - 5, window - 6, exhaust for the displacement diffuser - 7, exhaust for the mixing diffusers -8),[8]

The measuring positions were located at five poles in the chamber (see Figure 2), and recording readingsvertical distributions for air velocity and temperature were measured,[8]

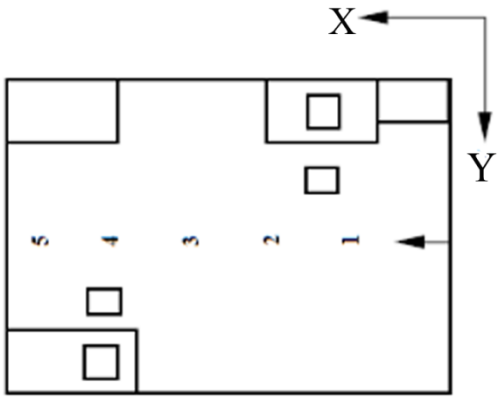

Figure 2. Measuring positions in the test room,[8].

3. MAHTEMATICAL MODELS

Three-dimensional incompressible turbulence of indoor air by turbulence model was simulated in this article [9]. To simplify the issue, the models were assumed as follows:

1) Indoor air was incompressible, invariable property, steady-state flow and coincidence with the basic assumption of Boussinesq.

2) Heat-transfer in walls was equable and it was considered as steady-state.

3) Air leakage was without consideration. The door and windows were assumed to be closed when air supplying and their sealing performance was good.

4) Glass scattering to solar radiation and the impact of interior heat-transfer surfaces were considered as constant heat flux.

The turbulence model, considering the influence of buoyant force, adopted two-equation Realizable k-ε and k-ω models with the wall-function method.

Continuity equation

$$\frac{\partial}{\partial x}(\rho u) + \frac{\partial}{\partial y}(\rho v) + \frac{\partial}{\partial Z}(\rho w) = 0 \quad \dots 1$$

X – direction (U momentum)

$$\frac{\partial}{\partial t}(\rho u) + \frac{\partial}{\partial x}(\rho u u) + \frac{\partial}{\partial y}(\rho u v) + \frac{\partial}{\partial z}(\rho u w) = -\frac{\partial p}{\partial x} + \frac{\partial}{\partial x}\left(\mu_e \frac{\partial u}{\partial x}\right) + \frac{\partial}{\partial y}\left(\mu_e \frac{\partial u}{\partial y}\right) + \frac{\partial}{\partial z}\left(\mu_e \frac{\partial u}{\partial z}\right) + \frac{\partial}{\partial x}\left(\mu_e \frac{\partial u}{\partial x}\right) + \frac{\partial}{\partial y}\left(\mu_e \frac{\partial v}{\partial x}\right) + \frac{\partial}{\partial z}\left(\mu_e \frac{\partial w}{\partial x}\right) \quad \dots 2$$

Y – direction (Y momentum):

$$\frac{\partial}{\partial t}(\rho v) + \frac{\partial}{\partial x}(\rho u v) + \frac{\partial}{\partial y}(\rho v v) + \frac{\partial}{\partial z}(\rho v w) = -\frac{\partial p}{\partial y} + \frac{\partial}{\partial x}\left(\mu_e \frac{\partial v}{\partial x}\right) \frac{\partial}{\partial y}\left(\mu_e \frac{\partial v}{\partial y}\right) + \frac{\partial}{\partial z}\left(\mu_e \frac{\partial v}{\partial z}\right) + \frac{\partial}{\partial x}\left(\mu_e \frac{\partial u}{\partial y}\right) + \frac{\partial}{\partial y}\left(\mu_e \frac{\partial v}{\partial y}\right) + \frac{\partial}{\partial z}\left(\mu_e \frac{\partial w}{\partial y}\right) - g(\rho - \rho_0) \quad \dots 3$$

Z – direction (W momentum):

$$\frac{\partial}{\partial t}(\rho w) + \frac{\partial}{\partial x}(\rho u w) + \frac{\partial}{\partial y}(\rho v w) + \frac{\partial}{\partial z}(\rho w w) = -\frac{\partial p}{\partial z} + \frac{\partial}{\partial x}\left(\mu_e \frac{\partial w}{\partial x}\right) + \frac{\partial}{\partial y}\left(\mu_e \frac{\partial w}{\partial y}\right) + \frac{\partial}{\partial z}\left(\mu_e \frac{\partial w}{\partial z}\right) + \frac{\partial}{\partial x}\left(\mu_e \frac{\partial u}{\partial z}\right) + \frac{\partial}{\partial y}\left(\mu_e \frac{\partial v}{\partial z}\right) + \frac{\partial}{\partial z}\left(\mu_e \frac{\partial w}{\partial z}\right) \quad \dots 4$$

And energy conservation equation

$$\frac{\partial}{\partial t}(\rho T) + \frac{\partial}{\partial x}(\rho u T) + \frac{\partial}{\partial y}(\rho v T) + \frac{\partial}{\partial z}(\rho w T) = \frac{\partial}{\partial x}\left(\Gamma_e \frac{\partial \mathrm{T}}{\partial \mathrm{x}}\right) + \frac{\partial}{\partial y}\left(\Gamma_e \frac{\partial \mathrm{T}}{\partial \mathrm{y}}\right) + \frac{\partial}{\partial z}\left(\Gamma_e \frac{\partial \mathrm{T}}{\partial z}\right) + S_T \quad \dots 5$$

The modeled transport equations for k and ε in the realizable (k, ε) model are

k - equation

$$\frac{\partial}{\partial t}(\rho k) + \frac{\partial}{\partial x_j}(\rho k U_j) = \frac{\partial}{\partial x_j}\left[\left(\mu + \frac{\mu_t}{\sigma_k}\right)\frac{\partial k}{\partial x_j}\right] + G_k + G_b - \rho\varepsilon - Y_M + S_k \quad \dots 6$$

ε - equation

$$\frac{\partial}{\partial t}(\rho \varepsilon) + \frac{\partial}{\partial x_j}(\rho \varepsilon U_j) = \frac{\partial}{\partial x_j}\left[\left(\mu + \frac{\mu_t}{\sigma_\varepsilon}\right)\frac{\partial \varepsilon}{\partial x_j}\right] + \rho C_1 S_\varepsilon - \rho C_2 \frac{\varepsilon^2}{k+\sqrt{v\varepsilon}} + C_{1\varepsilon}\frac{\varepsilon}{k} C_{3\varepsilon} G_b + S_\varepsilon \quad \dots 7$$

k - equation

$$\frac{\partial}{\partial t}(\rho k) + \frac{\partial}{\partial x_i}(\rho k U_i) = \frac{\partial}{\partial x_j}\left[\Gamma_k \frac{\partial k}{\partial x_j}\right] + \tilde{G}_k + -Y_k + S_k \quad \dots 8$$

ω - equation

$$\frac{\partial}{\partial t}(\rho \omega) + \frac{\partial}{\partial x_j}(\rho \omega U_i) = \frac{\partial}{\partial x_j}\left[\Gamma_\omega \frac{\partial \omega}{\partial x_j}\right] + G_\omega - Y_\omega + D_\omega + S_\omega \quad \dots 9$$

Where all constant in equations (6-9) are found in Fluent user's guide,[10].

4. BOUNDARY CONDITION

At air inlet the boundary condition for velocity and temperature listed in Table 1 for four type of diffuser.

Table 1 boundary condition for inlet,[8]

Diffuser	ACH(kg/s)	T_{supply}	T_{exhust}
Displacement	5.0 (0.0768)	13.0	22.2
Slot (Linear)	9.2 (0.1410)	16.3	21.4
Square Ceiling	4.9 (0.0750)	14.5	24.1
Grille	5.0 (0.0768)	15.1	24.5

In addition to the internal heat gains as shown in Table 2, there is 341 Btu/h (100 W) to 580 Btu/h (170 W) of cooling load from the window that depends on the diffuser type and ventilation rate

.

Table 2. Internal heat sources in the environmental chamber,[8]

Internal Heat Sources	Btu/hr (W)
Each human simulator	256 (75)
Computer 1	368 (108)
Computer 2*	590 (173)
Each fluorescent lamp	116 (34)
TOTAL	1935 (567)

* The one close to the window

$$k_0 = 1.5(T_i \times U_0)^2 \ldots 10$$

$$\varepsilon_0 = \frac{C_\mu^{3/4} k_0^{3/2}}{l_0} \quad \ldots 11$$

where U_0 is the supply velocity, T_i is the turbulence intensity, C_μ= 0.09 is the empirical constant, and l_0=0.1L is the length scale. L normally equals to the characteristic length of the diffuser, such as the width of the slot diffuser,[8].

5. NUMERICAL COMPUTATION

The computational meshes were portioned with rectangular coordinate system and describing the mesh model using the Gambit 2.2.30 and the step-size of the main meshes was 0.1m on the directions of three coordinate axes. The meshes were made at human bodies, objects around, air-inlets and air-outlets.

6. DISCRETIZATION SCHEMES

The second-order upwind scheme is used for the discretization of the convection terms and the second order. For the discretization of the pressure, the PRESTO! (PREssureSTaggering Option) scheme is used. The SIMPLE scheme and SIMPLEC scheme is used for the pressurevelocity coupling[10],[11].

7. RESULTS AND DISCUSSION

7.1 Experimental Results

The four test cases are taken from a recent report ASHRAE RP-1009 "SimplifiedDiffuser Boundary Conditions for Numerical Room Airflow Models" (Chen et al. 2001)[8], both test caseshave the same internal configuration including two human simulators, two computers, two cabinets, twotables (for PC) and four fluorescent lamps. The differences between the test cases are the type andposition of the inlet diffuser and the outlet, and the ventilation rate.

7.2 Numerical Results

7.2.1 Displacement Ventilation

In Figure3 and 4 a comparison of the predicted air velocity and temperature profiles using Realizable k-ε and SST k-ω model with experiment measurements is given, respectively. The predicted temperatures have some discrepancies with measured data near ceiling and floor, this may be a consequence of the imposed thermal boundary conditions at the ceiling and the floor in the experiment, the measured temperature near the diffuser (17.42°C at X=0.8m) has 3°C difference with the temperature near the West wall and (20.43°C at X=4.36m) has 1.313 °C difference at the floor, by imposing an averaged temperature (23°C) at the floor thus the predicted temperature is lower than the measured value. From Figure4, it can be seen that the predicted temperatures near the floor are generally lower than the measured ones. Despite the discrepancies, the vertical temperature gradient in the middle of the room is well predicted, which is an important parameter influencing thermal comfort for displacement ventilation.

7.2.2 Ceiling Slot Ventilation

The Figure5 and 6 gives a comparison of the predicted air velocity and temperature profiles using Realizable k-ε and SST k-ω models with experimental data, respectively. It can be seen that the predicted profiles correspond reasonably well with measured ones. In Figure 5 and 6, the predicted air velocity and temperature profiles at X=1.78m, and 2.51m have some big discrepancies compared with measured data in the ceiling region, this is likely due to the momentum model used for the inlet diffuser, because in Chen et al. 2001 [8] when using the momentum model for the diffuser, they obtained the same results for the predicted temperature profiles, the discrepancies at X=3.36 still exists. When it is used with the k-ε or k-ω models, it may also contribute to some degree to the discrepancies between the predicted temperature profiles and the measured ones. In the occupied zone, thus the prediction using the model for the diffuser is acceptable for practical purposes.

7.2.3 Ceiling Square Ventilation

Simulations are carried out with the Realizable k-ε, the SST k-ω modelsand with Box and Momentum methods published. Figure 7 and 8 gives a comparison of the predicted air velocity, temperature profiles using Realizable k-ε and SST k-ω models with experimental data, respectively. It can be seen that the predicted profiles correspond reasonably well with measured ones. In Figure 7, the predicted air velocity profiles at X=0.8m, have some big discrepancies compared with measured data in the ceiling region, and in Figure 8, the predicted air temperature at X=0.8m have some big discrepancies compare with measured date in the floor region, this is due to selected model used for the inlet diffuser, It is noted that the prediction that we have it better than the way from Box and Momentum method.

7.2.4 Grille Ventilation

The simulations have used both he Realizable k-ε and the SST k-ω models for the diffuser. The calculated and measured velocities are presented in Figure 9 for both methods. The results show that the maximum velocity at the jet region in the middle section. However, the calculated velocity profile presented for pole 1 shows a much higher maximum jet velocity. In fact, the measured jet velocity profile in that area is asymmetric due to the possible asymmetric discharge angle. Figure 10 presents calculated and measured temperature profiles. However, the measured jet was closer to the ceiling than the calculated one.

8. CONCLUSION

In this work simulated cooling for the enclosed room. Numerical analysis based on finite volume method is used to solve three-dimensional steady flow with used k-ε and k-ω turbulent models in resulting temperature distribution and air velocity. The results showed a good comparison with the results of the research [ASHRAE RP-1009], and this is something which demonstrates the great potential of the theoretical analysis method used in the search to detect design flaws for air diffusers and locations.

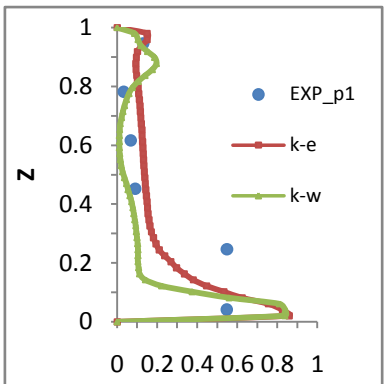

a

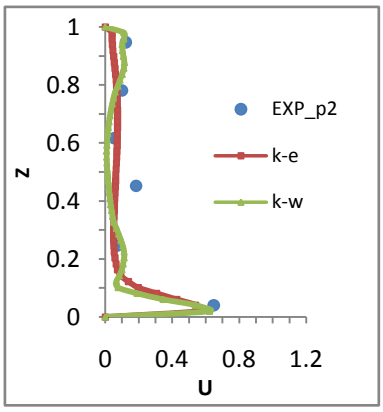

b

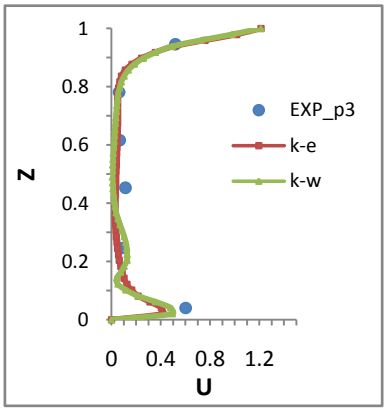

c

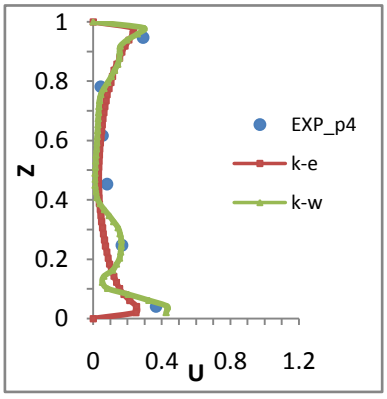

d

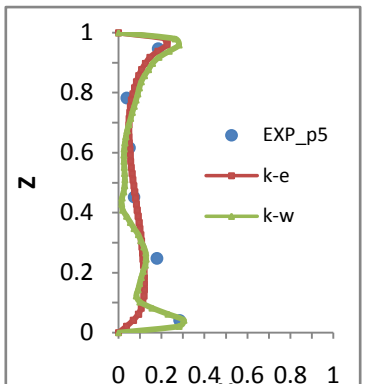

e

Figure3Comparison of predicted mean air speed profiles with measurementsRealizable k-ε and SST k-ω models, Z=height/total room height (H), U=velocity/supply velocity (U_0), H=2.43m, U_0=0.35m/s

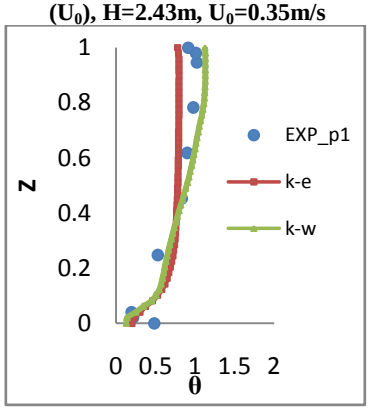

a

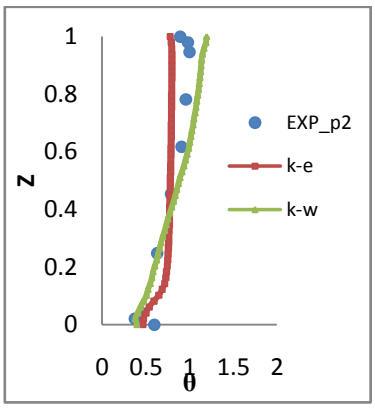

b

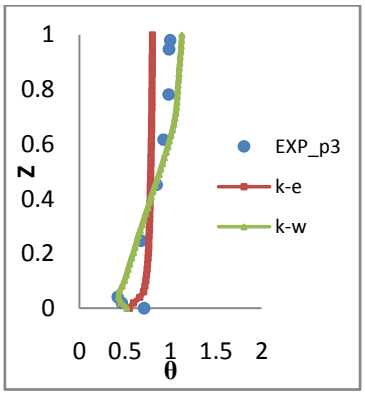

c

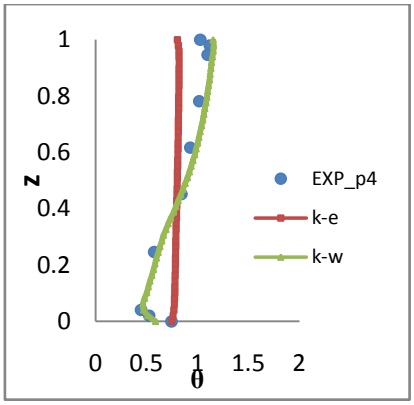

d

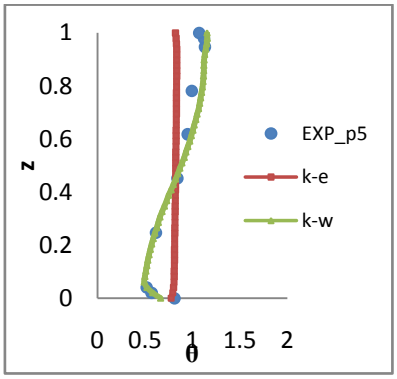

e

Figure 4Comparison of predicted temperature profiles with measurements with Realizable k-ε and SST k-ω models, Z=height/total room height (H), θ=(T-Tin/Tout-Tin), H=2.43m, Tin=13.0°C, Tout=22.2°C

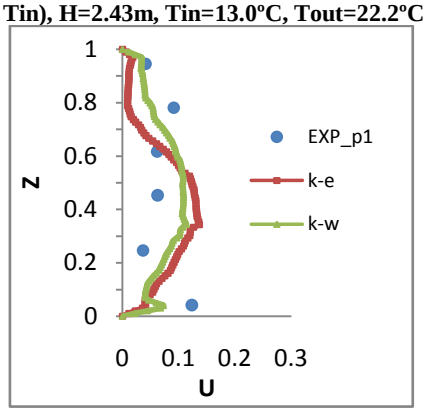

a

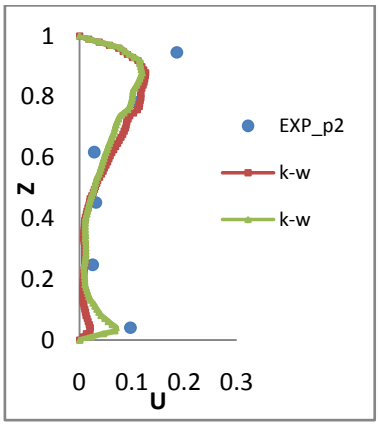

b

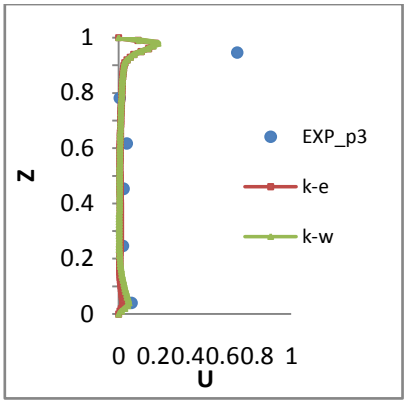

c

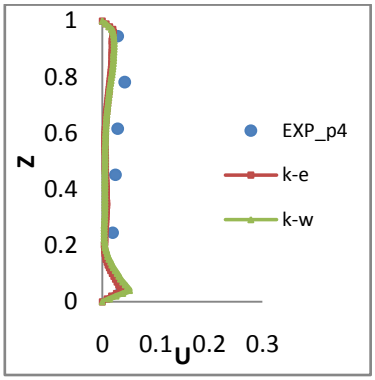

d

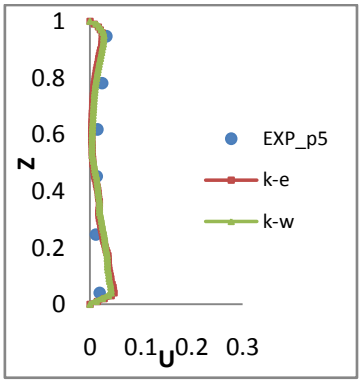

e

Figure 5Comparison of predicted mean air speed profiles with measurements Realizable k-ε and SST k-ω models, Z=height/total room height (H), U=velocity/supply velocity (U_0), H=2.43m, U_0=3.9m/s

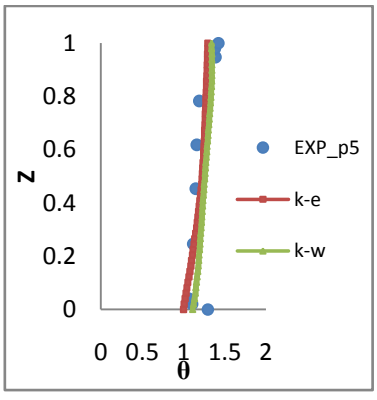

a

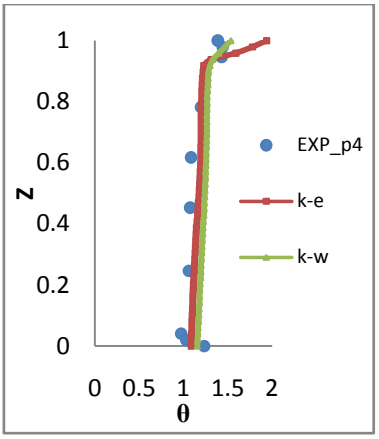

b

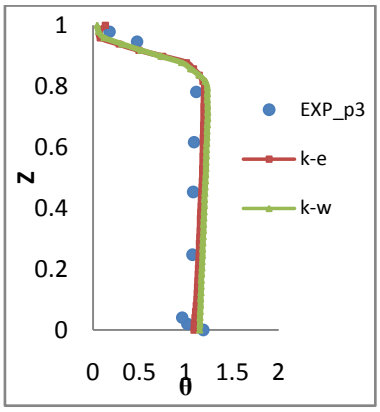

c

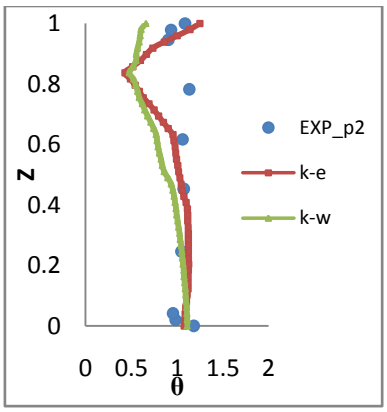

d

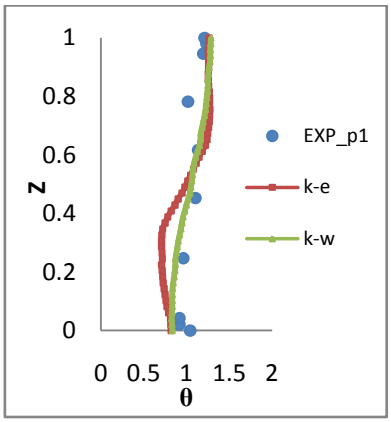

e

Figure 6Comparison of predicted temperature profiles with measurements Realizable k-ε and SST k-ω models, Z=height/total room height (H), θ=(T-T_{in}/T_{out}-T_{in}), H=2.43m, Tin=16.3ºC, Tout=21.4ºC

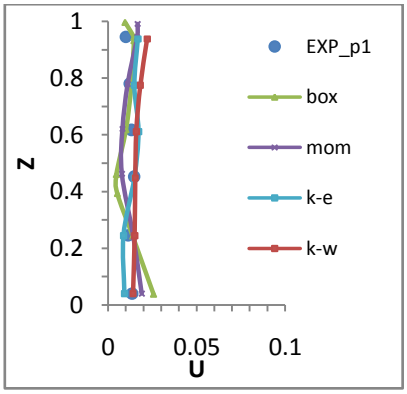

a

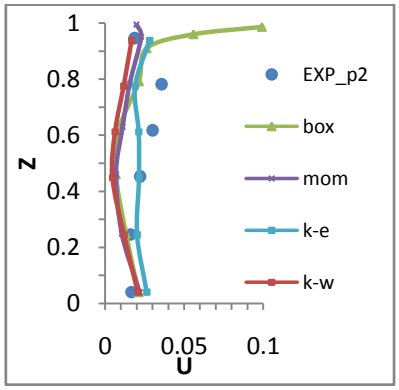

b

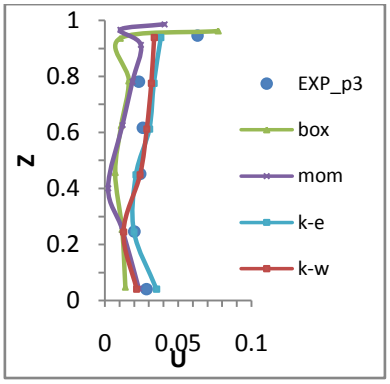

c

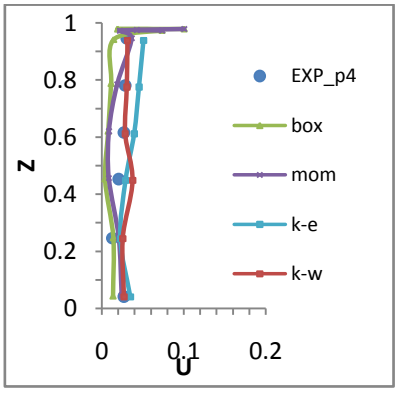

d

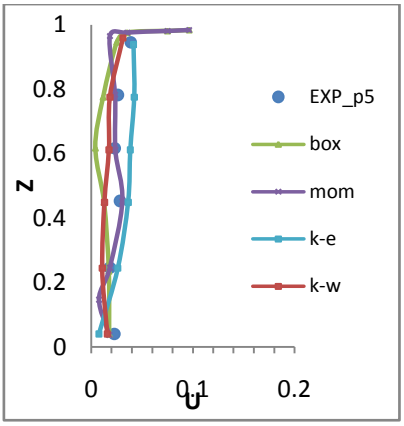

e

Figure 7Comparison of predicted mean air speed profiles with measurements Realizable k-ε and SST k-ω models compared with box and momentum, Z=height/total room height (H), U=velocity/supply velocity (U_0), H=2.43m, U_0=5.2m/s

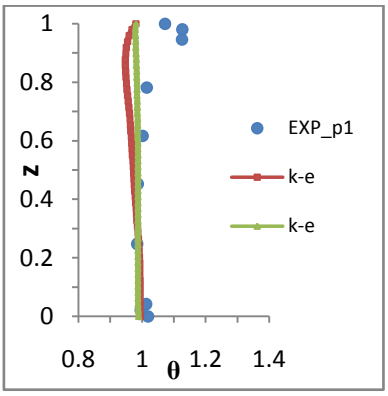

a

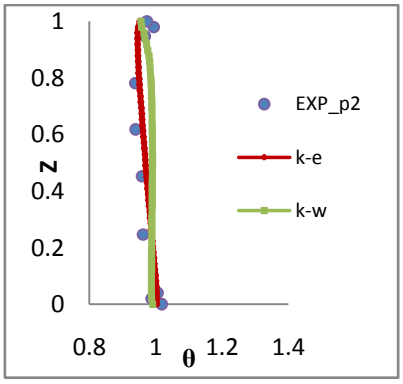

b

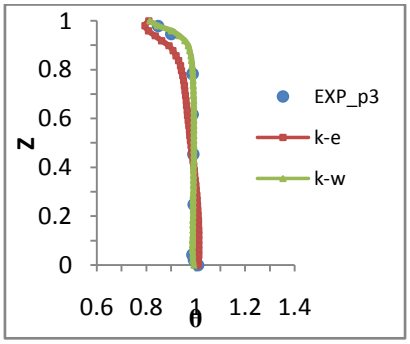

c

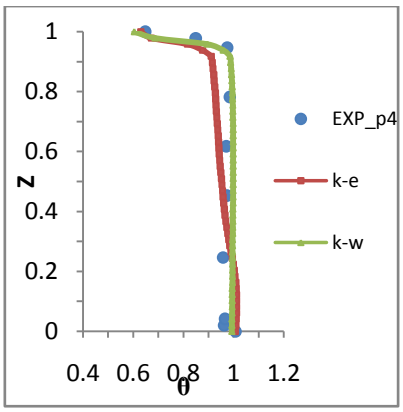

d

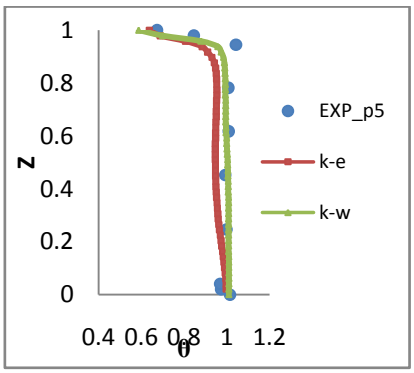

e

Figure 8Comparison of predicted temperature profiles with measurements Realizable k-ε and SST k-ω models compared with box and momentum, Z=height/total room height (H), θ=(T-T_{in}/T_{out}-T_{in}), H=2.43m, Tin=14.5°C, Tout=24.1°C

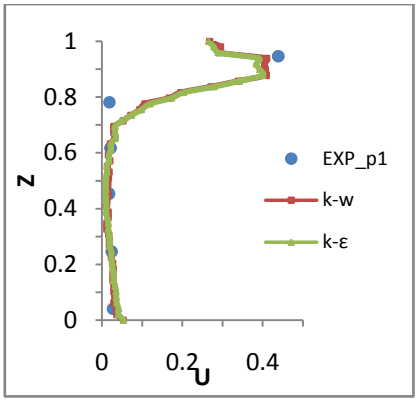

a

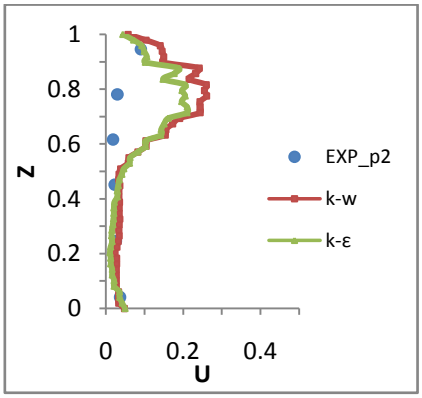

b

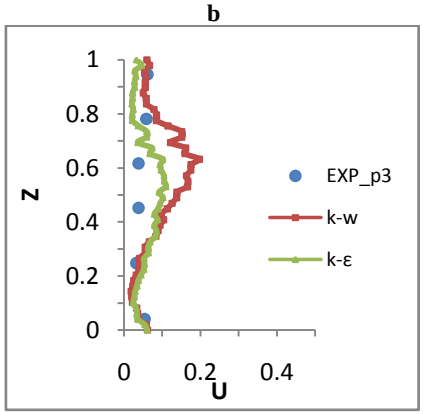

c

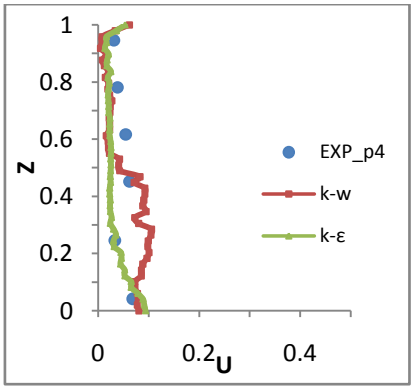

d

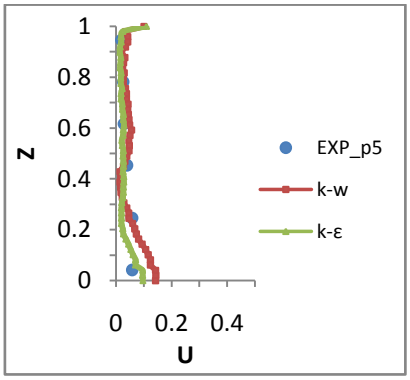

e

Figure 9Comparison of predicted mean air speed profiles with measurements Realizable k-ε and SST k-ω models,*Z=height/total room height (H), U=velocity/supply velocity (U_0), H=2.43m, U_0=2.7m/s*

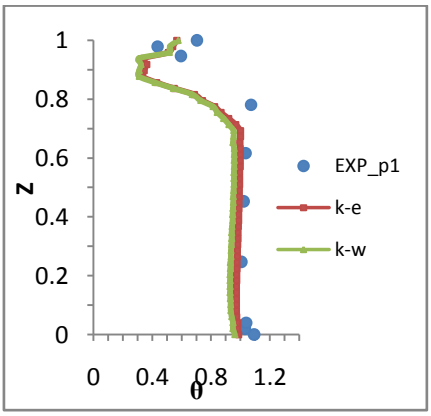

a

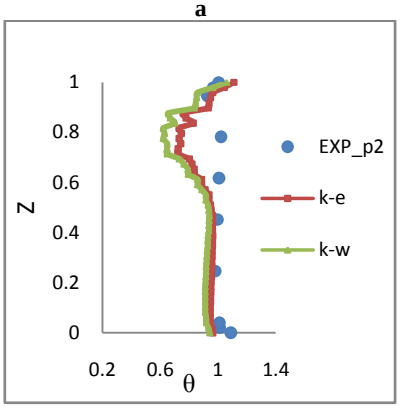

b

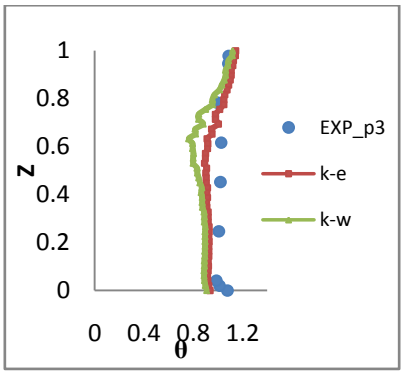

c

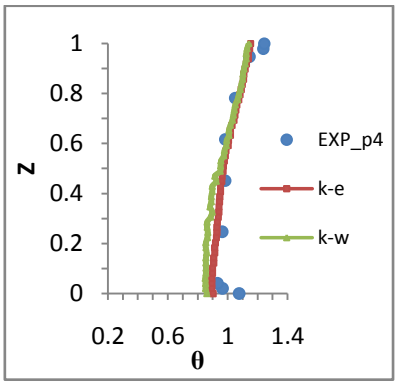

d

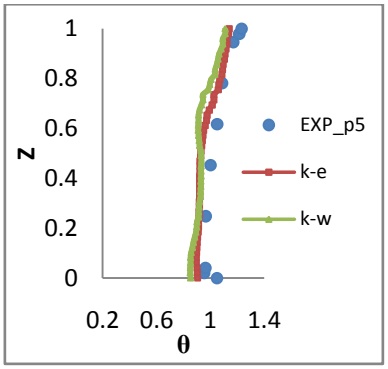

e

Figure 10Comparison of predicted temperature profiles with measurements Realizable k-ε and SST k-ω models compared with box and momentum, *Z=height/total room height (H), θ=(T-T_{in}/T_{out}-T_{in}), H=2.43m, Tin=15.1℃, T_{out}=24.5℃*

9. NOMENCALTURE

u-v-w	Velocity component in x-y-z diraction
μ_e	The effective viscosity coefficient
ρ_o	The density at reference temperature
$\Gamma_e, \Gamma_k, \Gamma_\omega$	The effective diffusion
k	Kinetic energy
ε	Dissipation rate of turbulence energy
ω	Turbulence frequency of energy
μ_t	The turbulent or eddy viscosity
G_k,	The generation of turbulence kinetic energy due to the mean velocity gradient
G_b	The generation of turbulence kinetic energy due to the buoyancy
Y_m	The contribution of fluctuation dilution incompressible turbulent
S_ε, S_k, S_ω, S_T	User-define source terms
C_1, C_2, $C_{3\varepsilon}$, σ_3, σ_k,	Constant
Y_k, Y_ω	The dissipation of k & ω due turbulence
G_ω	The generation of ω
D_ω	The cross-diffusion term

10. REFERENCES

[1] Skovgaard, M., and Nielsen, P.V. 1991. Modelling complex inlet geometries in CFD -Applied to air flow in ventilated rooms,Proc. of 12th AIVC Conference, Vol.3, P.P.183-200.

[2] Srebric J. Chen Q. 2002. Simplified Numerical Models for Complex Air Supply Diffusers. HVAC&R Research 8(3) P.P 277-294.

[3] M. Cehlin ,B.Moshfegh. 2010, Numerical modeling of a complex diffuser in a room with displacement ventilation, Building andEnvironment45 P.P.2240-2252.

[4] Zhao B. LiX. YanQ. 2003, A simplified system for indoor airflow simulation. Building and Environment 38.P.P. 543 – 552.

[5] Lee, K.S., Zhang, T., Jiang, Z., and Chen, Q. 2009. Comparison of airflow and contaminant distributionsin rooms with traditional displacement ventilation and under-floor air distribution systems,ASHRAE Transactions, 115(2).

[6] Yun-Chun Tung, Yang-Cheng Shih, Shih-Cheng Hu. 2009.Numerical study on the dispersion of airborne contaminants from an isolation room in the case of door opening. Applied Thermal Engineering. 29.P.P. 1544–1551.

[7] N. El Gharbi, R. Absi, A. Benzaoui, 2011. Effect of Different Near-Wall Treatments on Indoor Airflow Simulations. Journal of Applied Fluid Mechanics, Vol. 4, No. 5, P.P. 63-70.

[8] Chen, Q. and Srebric, J. 2001. Simplified diffuser boundary conditions for numericalroom airflow models. Final Report for ASHRAE RP-1009, 181 pages,Department of Architecture, Massachusetts Institute of Technology, Cambridge,MA.

[9] Awbi H. B. 2003. Ventilation of Buildings. Spon Press.

[10] FLUENT 6.3 Documentation. 2006.www.Fluent.com.

[11] PatankarS.V. 1980. Numerical Heat Transfer and Fluid Flow. Hemisphere Washington DC.